The thermal structure of volcanic passive margins

Supplementary information

John J. Armitage and Jenny S. Collier

Governing equations

The numerical model is developed from an early version of the open source Stokes flow solver CitCom. This is a finite element numerical model that solves for the conservation of energy, mass and momentum for flow that has a viscosity that varies over five orders of magnitude (Moresi and Solomatov, 1995). The key equation is the conservation of momentum,

$$\frac{-\partial \tau_{ij}}{\partial x_j} + \frac{\partial p}{\partial x_i} = -\Delta \rho g \lambda_i$$

where upward flow, x_2 in the tensor notation used above, is in the negative direction, τ is the deviatoric stress tensor, p, is pressure, $\Delta\rho$, is the change in density, g, is the acceleration due to gravity, and λ_i, is a unit vector in the vertical direction. The momentum balance is key because both temperature and melt production in the upper mantle will affect the change in density, $\Delta\rho$, and the viscosity that feeds into the stress tensor, τ.

We write the change in density as a function of temperature and melt production as follows:

$$\Delta\rho = \rho_0(\alpha\Delta T + \beta F + \gamma\phi)$$

where ρ_0 is the reference rock density; α is the coefficient of thermal expansion; $\Delta T = T - T_m$, is the temperature difference between the local temperature and the reference mantle potential temperature; β is a coefficient that sets the magnitude of density changes due to accumulated depletion, F, which is equivalently the accumulated mass fraction of melt generated; γ is a coefficient that sets the magnitude of density change due to the retained melt fraction by volume, φ or porosity. As defined, an increase in melt production acts in two ways to change the density and hence the viscous flow, first by increasing the accumulated compositional depletion and second through the effect of buoyant retained melt in the mantle. The change in melt depletion is tracked using a hypothetical tracer X that always partitions into the melt, such that it is related to F by $X(1-F)=1$ (Scott, 1992).

The deviatoric stress, τ, is a function of viscosity, η:

$$\tau_{ij} = 2\eta\epsilon_{ij}$$

where ε_{ij} is strain rate. Melt generation very likely affects the viscosity of the mantle. We include two parametrised affects:

(1) Strengthening due to the removal of mantle volatiles (Hirth and Kohlstedt, 1996; Karato and Jung, 2003; Fei et al., 2013). We assume that the removal of mantle volatiles and in particular water leads to a two order of magnitude increase in the strength of the upper mantle. Therefore we include a pre-factor, χ_w, which is equal to one until 2% mass fraction of melt is generated. After this percentage χ_w = 100.

(2) Weakening of the mantle matrix due to melt retained within the grain boundaries (e.g. Kelemen et al., 1997). This weakening effect is included through a pre-factor, $\chi_\varphi = \exp(-45\phi)$.

The rheology is then given by,

$$\eta = A\chi_w\chi_m exp\left(\frac{E+pV}{nRT}\right)\dot{I}_2^{\frac{1-n}{n}}$$

where *E* and *V* are the activation energy and volume, *R* is the gas constant, *I* is the second invariant of the strain rate, *n* is the stress exponent and finally *A* is a scaling parameter (see for example Christensen, 1992; Armitage et al., 2013). The numerical model therefore captures the buoyant, or sometimes termed active, upwelling of mantle due to the generation of melt. It also captures the competing effects of a reduction in viscosity due to melt generation and an increase in viscosity due to the depletion of the solid mantle matrix.

Model set-up

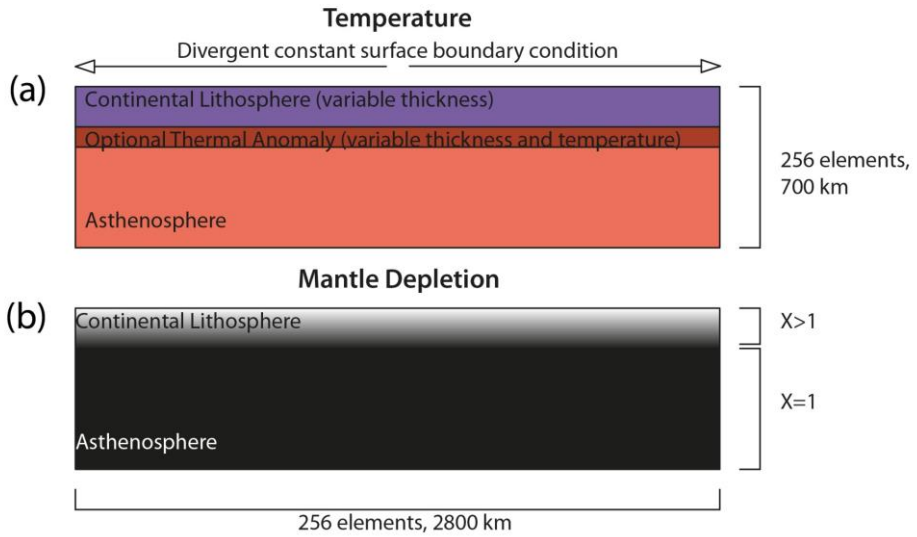

Figure A1 Example starting model. In all runs the starting lithosphere is assumed to be a uniform thickness layer. (a) Initial temperature within the upper mantle, which includes the asthenosphere and lithosphere. The temperature at the base of the model at 700 km depth is either 1250, 1275 or 1315 °C. The 'hot layer' is either 0, 25, or 50 km thick and 100 or 200 °C hotter than the mantle potential temperature. (b) Initial melt residue X within the upper mantle, where the lithosphere is set to be melt depleted (X>1) and therefore buoyant.

We solve the system of equations outlined above within a Cartesian box that has an aspect ratio of 4:1, where the depth of the box is 700 km. The continental lithosphere is a conductive layer and is defined by a linear increase in both temperature and trace element

X with depth to simulate an increase in depletion and make it buoyant (Figure A1). The thickness of the starting lithosphere can vary and in most of our work we set this to values provided by surface wave studies (e.g. McKenzie et al., 2015).

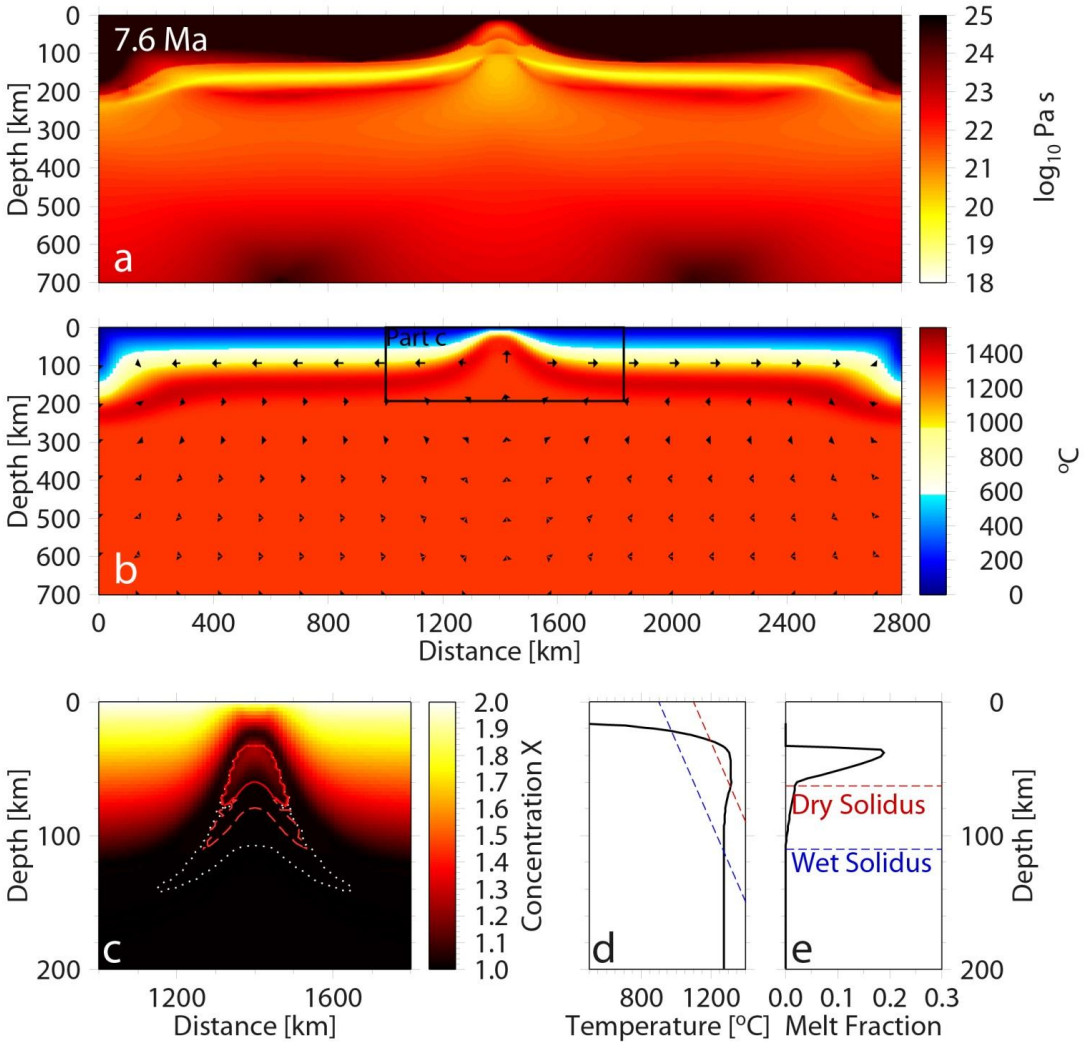

Figure A2 Example model results after 7.6 Ma of symmetric extension at a half spreading rate of 20 mm/yr with an initial 50 km thick 200 ^{0}C thermal anomaly below the initial 125 km thick lithosphere. In this example the mantle potential temperature is 1275 ^{0}C. The model is close to the point of continental breakup. (a) Model viscosity. (b) Model temperature and vectors of solid mantle creep. (c) Mantle depletion in the region of breakup, along with the extent of the melt region (white dots) and 1% and 2% melt fraction contours (dashed and solid red lines, respectively). (d) A mantle geotherm through the centre of spreading (x=1400 km) and the dry and wet solidus (red and blue dashed lines respectively). (e) The melt fraction with depth profile through the centre of spreading.

We impose extension through a divergent upper boundary velocity condition. This divergence can stop at any time and then restart with a centre of extension at the same place or shifted laterally to simulate real rift histories. All the other sides of the 2-D box are of free slip. Once the model is started the applied the divergent velocity (extension) thins the lithosphere and causes the flow in the asthenosphere to start. At any given time step

the conditions for melting are tested, initially assuming a wet solidus, but after 2% melting a dry solidus (Figure A2).

In the model the temperature at the top surface is fixed at 0° C and at the base it is held fixed at the imposed asthenospheric temperature. To define a 'normal' model asthenospheric temperature we can compare model predicted steady state magmatic crust thickness with the average mid-ocean ridge thickness of 7±1 km (Bown and White, 1995). Such a thickness is achieved for the range of 1300 to 1350 °C depending on the model rate of extension (Nielsen and Hopper, 2004; Armitage et al., 2008; Armitage et al., 2011). As our model assumes that all melt that is generated is extracted, it will over-estimate 'normal' mid-ocean ridge melt thickness and therefore potentially under-estimate asthenospheric temperature (Behn and Grove, 2015). The side temperature boundary conditions are of zero flux. To explore the effect of a change in the mantle temperature we either introduce a thermal anomaly (either before the start of extension or at any point during the model run) or increase the temperature of the whole asthenosphere (Figure A1). Once the thermal properties of the asthenosphere and/or the hot layer are established they only change due to model evolution e.g. there is no replenishment of the hot layer by addition of hot material from the sides or below.

Once the model is started the applied the divergent velocity (extension) thins the lithosphere and causes the flow in the asthenosphere to start. At any given time step the conditions for melting are tested, initially assuming a wet solidus, but after 2% melting a dry solidus (Figure A2). To compare with observations we can calculate the following properties of the igneous rocks formed by the melting (i) its thickness, which is calculated as an integral of the melt production rate assuming all melt that is generated is erupted at the centre of extension (Ito et al., 1996); (ii) its major element oxide and Rare Earth Element (REE) composition (Armitage et al., 2008; Armitage et al., 2011); and (iii) its seismic P-wave velocity, which is calculated from the major element oxide composition (Behn and Kelemen, 2003). In the pre-breakup situation we can also calculate the seismic S-wave velocity of the upper mantle accounting for the effects of attenuation and melt retention (Goes et al., 2012; Armitage et al., 2015).

References

Armitage, J. J., J. S. Collier, T. A. Minshull & T. J. Henstock, 2011. Thin oceanic crust and flood basalts: India-Seychelles breakup. *Geochemistry Geophysics Geosystems* **12**. DOI: 10.1029/2010gc003316

Armitage, J. J., D. J. Ferguson, S. Goes, J. O. S. Hammond, E. Calais, C. A. Rychert & N. Harmon, 2015. Upper mantle temperature and the onset of extension and break-up in Afar, Africa. *Earth and Planetary Science Letters* **418**, 78-90. DOI: 10.1016/j.epsl.2015.02.039

Armitage, J. J., T. J. Henstock, T. A. Minshull & J. R. Hopper, 2008. Modelling the composition of melts formed during continental breakup of the Southeast Greenland margin. *Earth and Planetary Science Letters* **269**, 248-258. DOI: 10.1016/j.epsl.2008.02.024

Armitage, J. J., C. Jaupart, L. Fourel & P. A. Allen, 2013. The instability of continental passive margins and its effect on continental topography and heat flow. *Journal of Geophysical Research-Solid Earth* **118**, 1817-1836. DOI: 10.1002/Jgrb.50097

Behn, M. D. & T. L. Grove, 2015. Melting systematics in mid-ocean ridge basalts: Application of a plagioclase-spinel melting model to global variations in major element chemistry and crustal thickness. *Journal of Geophysical Research-Solid Earth* **120**, 4863-4886. 10.1002/2015jb011885

Behn, M. D. & P. B. Kelemen, 2003. Relationship between seismic P-wave velocity and the composition of anhydrous igneous and meta-igneous rocks. *Geochemistry Geophysics Geosystems* **4**. DOI: 10.1029/2002gc000393

Bown, J. W. & R. S. White, 1995. Effect of finite extension rate on melt generation at rifted continental margins. *Journal of Geophysical Research-Solid Earth* **100**, 18011-18029. Doi 10.1029/94jb01478

Christensen, U. R., 1992. An Eulerian technique for thermomechanical modeling of lithospheric extension. *Journal of Geophysical Research* **97**, 2015. DOI: 10.1029/91jb02642

Fei, H. Z., M. Wiedenbeck, D. Yamazaki & T. Katsura, 2013. Small effect of water on upper-mantle rheology based on silicon self-diffusion coefficients. *Nature* **498**, 213-+. 10.1038/nature12193

Goes, S., J. Armitage, N. Harmon, H. Smith & R. Huismans, 2012. Low seismic velocities below mid-ocean ridges: Attenuation versus melt retention. *Journal of Geophysical Research-Solid Earth* **117**. DOI: 10.1029/2012jb009637

Hirth, G. & D. L. Kohlstedt, 1996. Water in the oceanic upper mantle: Implications for rheology, melt extraction and the evolution of the lithosphere. *Earth and Planetary Science Letters* **144**, 93-108. DOI: 10.1016/0012-821x(96)00154-9

Ito, G., J. Lin & C. W. Gable, 1996. Dynamics of mantle flow and melting at a ridge-centered hotspot: Iceland and the Mid-Atlantic Ridge. *Earth and Planetary Science Letters* **144**, 53-74. DOI: 10.1016/0012-821x(96)00151-3

Karato, S. I. & H. Jung, 2003. Effects of pressure on high-temperature dislocation creep in olivine. *Philosophical Magazine* **83**, 401-414. 10.1080/0141861021000025829

Kelemen, P. B., G. Hirth, N. Shimizu, M. Spiegelman & H. J. B. Dick, 1997. A review of melt migration processes in the adiabatically upwelling mantle beneath oceanic spreading ridges. *Philosophical Transactions of the Royal Society a-Mathematical Physical and Engineering Sciences* **355**, 283-318.

McKenzie, D., M. C. Daly & K. Priestley, 2015. The lithospheric structure of Pangea. *Geology* **43**, 783-786. 10.1130/G36819.1

Moresi, L. N. & V. S. Solomatov, 1995. Numerical investigation of 2D convection with extremely large viscosity variations. *Physics of Fluids* **7**, 2154-2162. DOI: 10.1063/1.868465

Nielsen, T. K. & J. R. Hopper, 2004. From rift to drift: Mantle melting during continental breakup. *Geochemistry Geophysics Geosystems* **5**. DOI: 10.1029/2003gc000662

Scott, D. R., 1992. Small-scale convection and mantle melting beneath midocean ridges *In* Mantle Flow and Melt Generation at Mid-Ocean Ridges. *Ed.* J. P. Morgan, D. K. Blackman and J. M. Sinton. 71 pp. 327-352.